HHS Public Access

Author manuscript

*RSC Adv*. Author manuscript; available in PMC 2017 July 08.

Published in final edited form as:

*RSC Adv*. 2016 July 8; 6(66): 61249–61253. doi:10.1039/C6RA10605F.

# Unusual Blue-Shifted Acid-Responsive Photoluminescence Behavior in 6-Amino-8-cyanobenzo[1,2-*b*]indolizines

**Victor K. Outlaw**[a], **Jiawang Zhou**[b], **Arthur E. Bragg**[b], and **Craig A. Townsend**[b]

[a]Department of Chemistry, University of Wisconsin–Madison, 1101 University Avenue, Madison, WI 53706, USA

[b]Department of Chemistry, The Johns Hopkins University, Remsen Hall, 3400 N. Charles Street, Baltimore, MD 21218, USA

## Abstract

6-Amino-8-cyanobenzo[1, 2-*b*]indolizines, a new class of photoluminescent materials, exhibit reversible pH-dependent optical properties characterized by an uncommon and dramatic blue shift in fluorescence emission when protonated. Acid titration and NMR spectroscopy experiments reveal that, rather than the anticipated N-protonation, C-protonation and loss of aromaticity is responsible for the observed photophysical changes. Efficient synthesis from indole-2-carboxaldehydes makes variously substituted versions of this nucleus readily available to tune optical and pH effects.

---

The photoluminescence of organic π–conjugated molecules has been of considerable interest owing to their utility as fluorescent probes and sensors.[1] Small molecules exhibiting fluorescence that can be modulated based on environmental factors, such as pH or the binding of specific analytes, are particularly valuable for their ability to report local microenvironments in solution, on surfaces, or within biological systems.[2] The fluorescence of polycyclic aza-aromatic compounds has been noted previously, and preparative methods and photophysical studies of these scaffolds remain areas of significant attention.[3] For example, several derivatives containing the 2-(4-pyridyl)-5-aryloxazole backbone have been investigated as donor–acceptor fluorescent pH probes.[4] For this class, a bathochromic shift in fluorescence was achieved at low pH, attributed to the increased withdrawing ability of the pyridyl moiety upon N-protonation. Similarly, Ihmels et al. described the synthesis of fluorescent anthryl-substituted benzoxazoles from anthracene-2-carboxylic acids, which demonstrated a red-shifted emission maximum when protonated at pH of 4–5.[5] Also, Tateno et al. described the synthesis of pentacyclic pyrrolo[1, 2-a]naphthylidine derivatives from N-arylcarbodiimides that exhibited a similar acid-inducible red shift of the fluorescence emission upon treatment with trifluoroacetic acid (TFA).[6] Finally, benzo[*a*]phenoxazine-based fluorophores, such as Nile Red and Nile Blue, utilize dialkylamino- substituents as electron donors to achieve pH-sensitive shifts in fluorescence.[7] For the vast majority of

---

Correspondence to: Craig A. Townsend.

Electronic Supplementary Information (ESI) available: synthesis and characterization data, experimental procedures, electronic structure calculations, UV-Vis and fluorescence emission spectra. See DOI: 10.1039/x0xx00000x

known indicators, acid-responsive changes in fluorescence involve redshifts in emission upon protonation; thus, in sensing or imaging applications protonated emission can be isolated (and neutral emission rejected) readily via long-pass filtration. Under highly acidic conditions, however, a reverse contrast could be desirable, requiring a hypsochromic (blue) shift in emission upon protonation. This could be achieved in systems susceptible to C-protonation that directly breaks conjugation of a polycycle. We report herein the preparation of a series of 6-amino-8-cyanobenzo[1, 2-*b*]indolizine fluorescent indicators, shown in Figure 1. We demonstrate that the pH-dependent shift is attributable to C-protonation of the heterocycle, thereby causing a break in conjugation and a blue-shift in emission.

Efficient routes have been reported recently to highly substituted 7-aminoindoles and 5-amino-N-fused heteroaromatic bicycles from pyrrole-3- and azole-2-carboxaldehydes, respectively.[8,9] These routes proceed by conjugate addition of trialkylphosphine to fumaronitrile, followed by proton reorganization and Wittig olefination. The resulting allylic nitrile is poised to undergo either Lewis acid-mediated Houben-Hoesch-type reaction on the more nucleophilic pyrrole C–2 to furnish the 7-aminoindoles, or base-catalysed deprotonation of the azolic N–H followed by cycloaromatization to the N-fused bicyclic structures. The application of this methodology to the synthesis of benzo[1, 2-*b*]indolizine tricyclic structures is not trivial. While pyrroles preferentially react with electrophiles at C–2, the more enamine-like indoles react at C–3, meaning that the intermediates for N–C and C–C cyclization would be identical. For this reason, divergent approaches to direct cycloaromatization to each nucleophilic site chemoselectively would be required.

To promote N–C cyclization, we employed conditions optimized for the formation of N-fused aromatic bicycles, as shown in Scheme 1.[9] Wittig reaction of commercially-available indole-2-carboxaldehyde with fumaronitrile and triethylphosphine generated intermediate **2a** in good yield. In situ deprotonation of the N–H, it was hypothesized, would allow for selective N–C ring closure and prevent formation of cyclization on carbon to form carbazole side products. To this end, addition of catalytic KOH to the crude Wittig reaction mixture afforded benzoindolizine **3a** in excellent yield. Interestingly, the yields of indolizines from pyrrole-2-carboxaldehydes described previously plateaued at approximately 75%, the stoichiometric yield from the E-isomer given the 3:1 E/Z ratio observed in the Wittig reaction. While Wittig reaction of the indole-2-carboxaldehyde afforded the same 3:1 E/Z ratio, a 90% yield of cyclized product was obtained, suggesting that the configurational isomers of alkene **2** exist in equilibrium prior to the cyclization step.

Using these conditions, a series of substituted benzoindolizine derivatives was synthesized. Indole-2-aldehydes substituted at various positions were submitted to the one-pot Wittig/cyclization sequence, and the yields and structures of benzoindolizine products are also shown in Scheme 1. Electron-donating groups at the 2-position of the benzoindolizine, such as alkyl and methoxy groups, were well tolerated, with good yields similar to the unsubstituted reaction. Electron-withdrawing substituents, however, such as the fluoro-substituted compound **3d** exhibited only moderate yields. This trend was also observed in the formation of the N-fused heteroaromatic bicycles. We believe that the electron-withdrawing moieties stabilize the indolide anion, thereby slowing cyclization. Finally, both donating and withdrawing substituents were not well tolerated at the C–4 position of the

benzoindolizine. This reduced reactivity is potentially due to $A^{1,3}$-strain that occurs between this substituent and the amine formed during the cyclization reaction.

With a series of 6-amino-8-cyanobenzo[1, 2-*b*]indolizines in hand, we next evaluated their photophysical properties. The neutral compounds exhibited similar UV-Vis absorption and fluorescence emission maxima, as summarized in Table 1. Electronic structure calculations with time-dependent density function theory (TD-DFT), found in the Supporting Information, correlate well with the observed UV-Vis data, and suggest that the lowest-energy absorption at approximately 440 nm stems from the HOMO to LUMO transition, whereas the more intense absorption band at 270 nm is associated with the transitions between the less delocalized HOMO-1 and HOMO-2 to LUMO. Of the compounds tested, **3d** exhibited the highest fluorescence quantum yield, indicating that the strongly electron withdrawing fluoro group significantly impacts the efficiency of competing non-radiative relaxation mechanisms. Conversely, electron donating substituents, such as the methoxy group of **3c**, did not significantly alter their optical properties.

To determine if this class of amino-substituted benzo[1, 2-*b*]indolizines exhibited acid-responsive fluorescence, their photophysical properties were evaluated at increasing concentrations of TFA; these results also summarized in Table 1. The UV-Vis spectra for titration of a methanolic solution of **3b** with TFA are shown Figure 2a. With increasing TFA concentration, the intensities of the absorption bands at 274 and 440 nm decrease, while a new band associated with the protonated **3b** centred at 370 nm concurrently emerges. Two isosbestic points at 297 and 398 nm manifest one major protonated product being formed during the TFA titration. Figure 2b presents the fluorescence emission spectra when excited at nm, resonant with absorption of the protonated **3b**. Upon addition of TFA, a new feature becomes apparent at nm with a quantum yield of 0.24. This acid-induced change can be easily visualized under UV radiation, where the colour of the **3b** solution changes from green to blue after acidification (Figure 3). The blue shift of the emission can be understood in connection with changes in absorption; upon protonation, the lowest absorption band shifts from 440 to 370 nm, indicating that the conjugation of the chromophore is partially broken (vida infra), and thus the band gap between the HOMO and LUMO increases. Accordingly, the emission of the protonated product should fall at higher energy. Compounds **3a**, **3d** and **3f** exhibited similar photophysical behaviour to **3b** upon protonation. The observed changes were reversible, as evidenced by recovery of the neutral **3b** in both UV-Vis and fluorescence spectra upon neutralization with triethylamine (See Supporting Information, Figure S4). This reversible change in fluorescence emission highlights the potential for this class of compounds as pH-sensing fluorophores.

In contrast, compound **3c** exhibits fairly different acid-responsive fluorescent behaviour. The UV-vis spectra of **3c** with TFA titration, shown in Figure 3c, strongly resemble the absorption changes observed for **3b**. However, unlike the increased fluorescence intensity seen for protonated **3b**, titration of compound 3c with TFA resulted in a sharp decrease in the fluorescence intensity, as shown in Figure 2d. Furthermore, protonated **3c** lacks the blue-shifted emission observed with **3b**. This disparity in the acid-responsive fluorescence of **3b** and **3c** can be observed in various solvents (Figure S5), and may be attributed to a

competitive excited-state process induced electronically by the presence of the methoxy substituent.

NMR analysis of a TFA-titrated solution of **3b**, shown in Figure 4, corroborates the existence of a single protonated intermediate. Interestingly, the $^{1}$H-NMR spectrum of the protonated species indicates that the protonation occurs not on the amino substituent (tautomeric structure **N**, Figure 5), but on a carbon atom in the C-ring with loss of aromaticity (tautomeric structures **T1** or **T2**, Figure 5). The amino – NH2 peak shifts downfield by 1.95 ppm and retains an integration of 2H. Meanwhile, the six aromatic C–H peaks previously observed convert to five in the protonated structure, with a methylene emerging upfield at 4.45 ppm that integrates to 2H. The loss of an aromatic C–H signal corresponds to an $sp^2$ to $sp^3$ hybridization change for a carbon within the **π**-conjugated system, which results in loss of aromaticity of the C-ring and is responsible for the change in optical properties. Quantum-chemical calculations performed at the CAM-B3LYP/6-31G*/PCM (methanol) level using the Gaussian 09 package[10] support our observations from NMR: the ground-state structure **N** is predicted to be 0.68 and 0.49 eV higher in energy than **T1** and **T2**, respectively.

In conclusion, we describe a route for the rapid synthesis of 6-amino-8-cyanobenzo[1, 2-*b*]indolizines from indole-2-carboxaldehydes. As hypothesized, these compounds exhibit acid-responsive fluorescent behaviour that can be manipulated according to the electronic nature of their substituents. NMR analysis indicates that the pH-dependent shift in fluorescence emission is due to protonation of carbon (likely structure **T1**, Figure 5) and loss of aromaticity in the C-ring, rather than the anticipated protonation of the amino moiety. The underlying photochemical principles governing the differences in behaviour with details of molecular structure are currently under investigation with ultrafast transient spectroscopies.

## Supplementary Material

Refer to Web version on PubMed Central for supplementary material.

## Acknowledgments

We are grateful for financial support from the National Institutes of Health research grant ES001670 (VKO, CAT). J.Z. gratefully acknowledges support through a Langmuir-Cresap fellowship. We also thank Dr. I. P. Mortimer (Johns Hopkins University, Department of Chemistry) for mass spectral analysis.

## Notes and references

1. a) Fernández-Suárez M, Ting AY. Nat. Rev. Mol. Cell Bio. 2008; 9:929–943. [PubMed: 19002208] b) Jung HS, Chen X, Kim JS, Yoon J. Chem. Soc. Rev. 2013; 42:6019–6013. [PubMed: 23689799] c) Li H, Fan J, Peng X. Chem. Soc. Rev. 2013; 42:7943–7920. [PubMed: 23845987] d) Zhu L, Yuan Z, Simmons JT, Sreenath K. RSC Advances. 2014; 4:20398–20343. [PubMed: 25071933] e) Guo Z, Park S, Yoon J, Shin I. Chem. Soc. Rev. 2014; 43:16–29. [PubMed: 24052190]
2. a) Pu L. Chem. Rev. 2004; 104:1687–1716. [PubMed: 15008630] b) Napolitano A, Panzella L, Leone L, d'Ischia M. Acc. Chem. Res. 2013; 46:519–528. [PubMed: 23270471] c) Carter KP, Young AM, Palmer AE. Chem. Rev. 2014; 114:4564–4601. [PubMed: 24588137] d) Basabe-Desmonts L, Reinhoudt DN, Crego-Calama M. Chem. Soc. Rev. 2007; 36:993–925. [PubMed: 17534482] e) Domaille DW, Que EL, Chang CJ. Nature Chem. Bio. 2008; 4:168–175. [PubMed: 18277978]

3. a) Liu B, Wang Z, Wu N, Li M, You J, Lan J. Chem.-Eur. J. 2012; 18:1599–1603. [PubMed: 22241666] b) Yang D-T, Radtke J, Mellerup SK, Yuan K, Wang X, Wagner M, Wang S. Org. Lett. 2015; 17:2486–2489. [PubMed: 25915087] c) Huanga X, Zhang T. Tetrahedron Lett. 2009; 50:208–211.d) Li W, Zhang Y-M, Zhang T, Zhang W, Li M, Zhang SX-A. J. Mat. Chem. C. 2016:1–6.e) Hilderbrand SA, Weissleder R. Chem. Commun. 2007; 26:2747–2743.f) Ooyama Y, Matsugasako A, Oka K, Nagano T, Sumomogi M, Komaguchi K, Imae I, Harima Y. Chem. Commun. 2011; 47:4448–4443.g) Liu D, Zhang Z, Zhang H, Wang Y. Chem. Commun. 2013; 49:10001–10003.h) Schmitt V, Moschel S, Detert H. Eur. J. Org. Chem. 2013; 25:5655–5669.i) Zhu L, Younes AH, Yuan Z, Clark RJ. J. Photoch. Photobio. A. 2015; 311:1–15.

4. a) Hall JH, Chien JY, Kauffman JM, Litak PT, Adams JK, Henry RA, Hollins RA. J. Heterocyc. Chem. 1992; 29:1245–1273.b) Diwu Z, Chen CS, Zhang C, Klaubert DH. Chem. Biol. 1999; 6:411–418. [PubMed: 10381401] c) Charier S, Ruel O, Baudin J-B, Alcor D, Allemand J-F, Meglio A, Jullien L. Angew. Chem. Int. Ed. Engl. 2004; 43:4785–4788. [PubMed: 15366087]

5. Ihmels H, Meiswinkel A, Mohrschladt CJ, Otto D, Waidelich M, Towler M, White R, Albrecht M, Schnurpfeil A. J. Org. Chem. 2005; 70:3929–3938. [PubMed: 15876081]

6. Tateno K, Ogawa R, Sakamoto R, Tsuchiya M, Otani T, Saito T. Org. Lett. 2014; 16:3212–3215. [PubMed: 24910923]

7. Jose J, Burgess K. Tetrahedron. 2006; 62:11021–11037.

8. Outlaw VK, Townsend CA. Org. Lett. 2014; 16:6334–6337. [PubMed: 25479249]

9. Outlaw VK, d'Andrea FB, Townsend CA. Org. Lett. 2015; 17:1822–1825. [PubMed: 25815402]

10. Frisch, MJ., et al., editors. Gaussian09. Revision A.1. Wallingford CT: Gaussian, Inc; 2009.

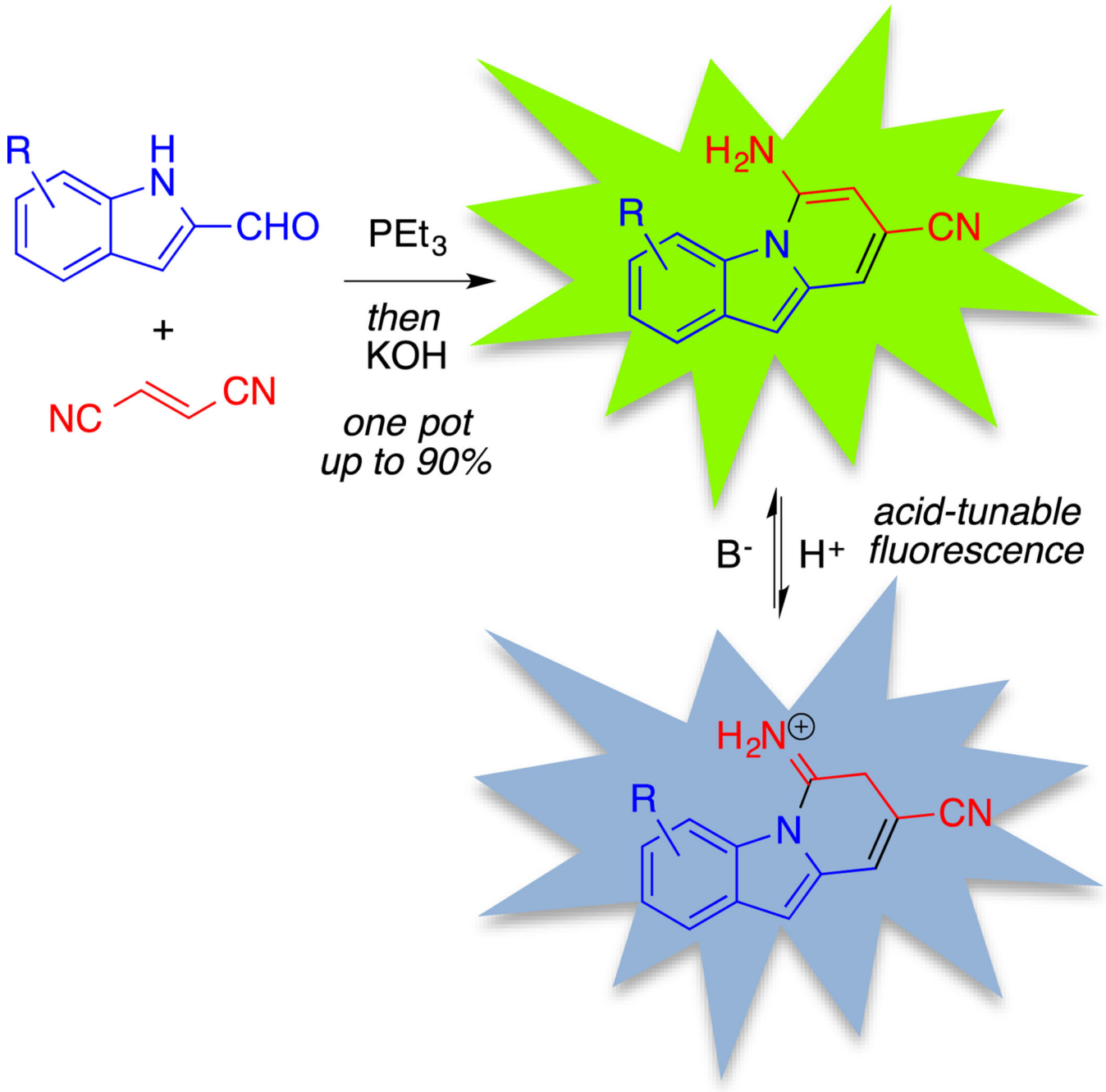


**Figure 1.**
Synthesis and observed pH-sensitive fluorescence of 6-amino-8-cyanobenzo[1, 2-*b*]indolizines.

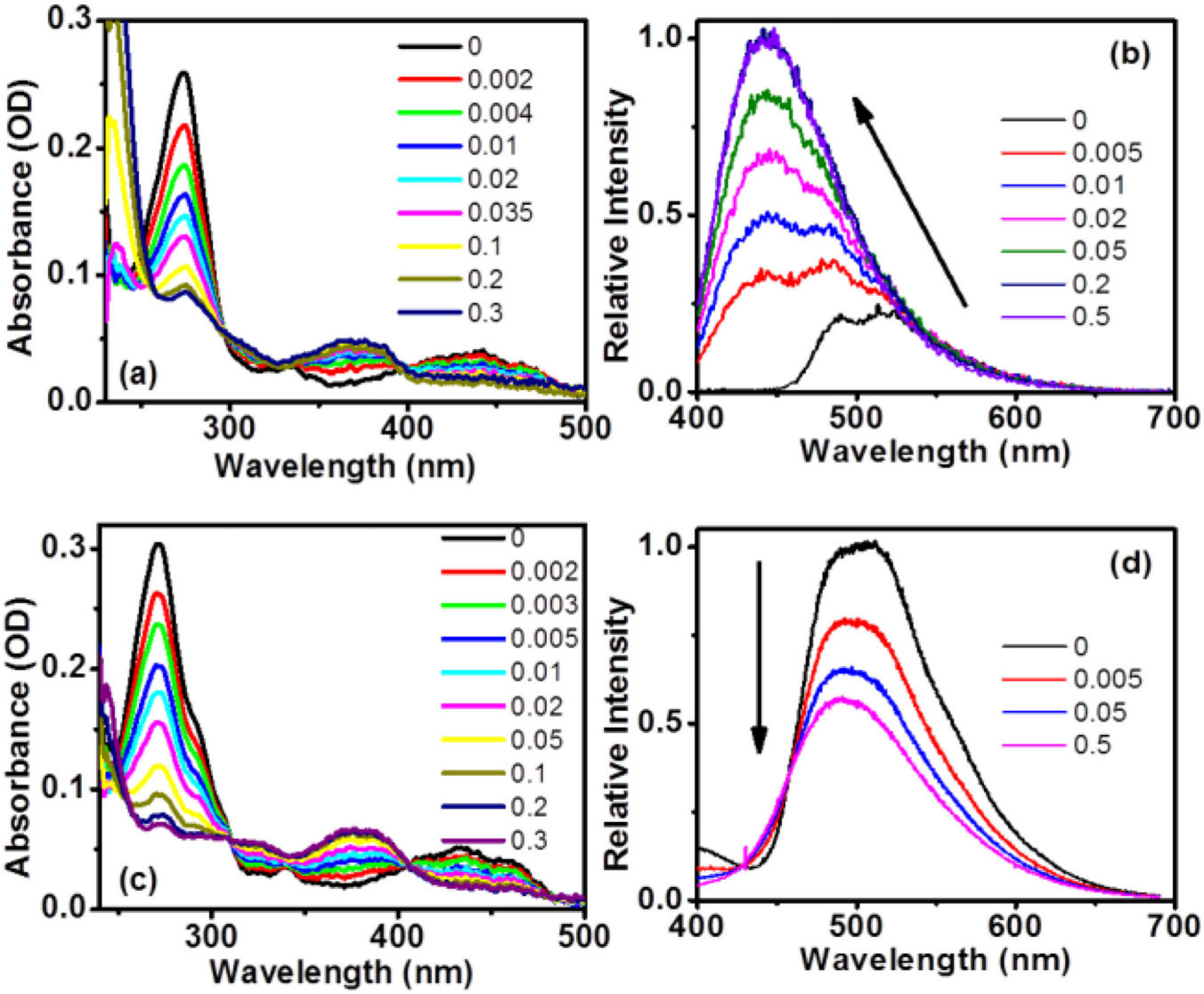


**Figure 2.**

(a) UV-Vis and (b) fluorescence spectra of **3b** and (c) UV-Vis and (d) fluorescence spectra of **3c** upon addition of TFA (vol %).The concentrations of **3b** and **3c** in fluorescence measurement are 5.4 μM and 2.8 μM, respectively.

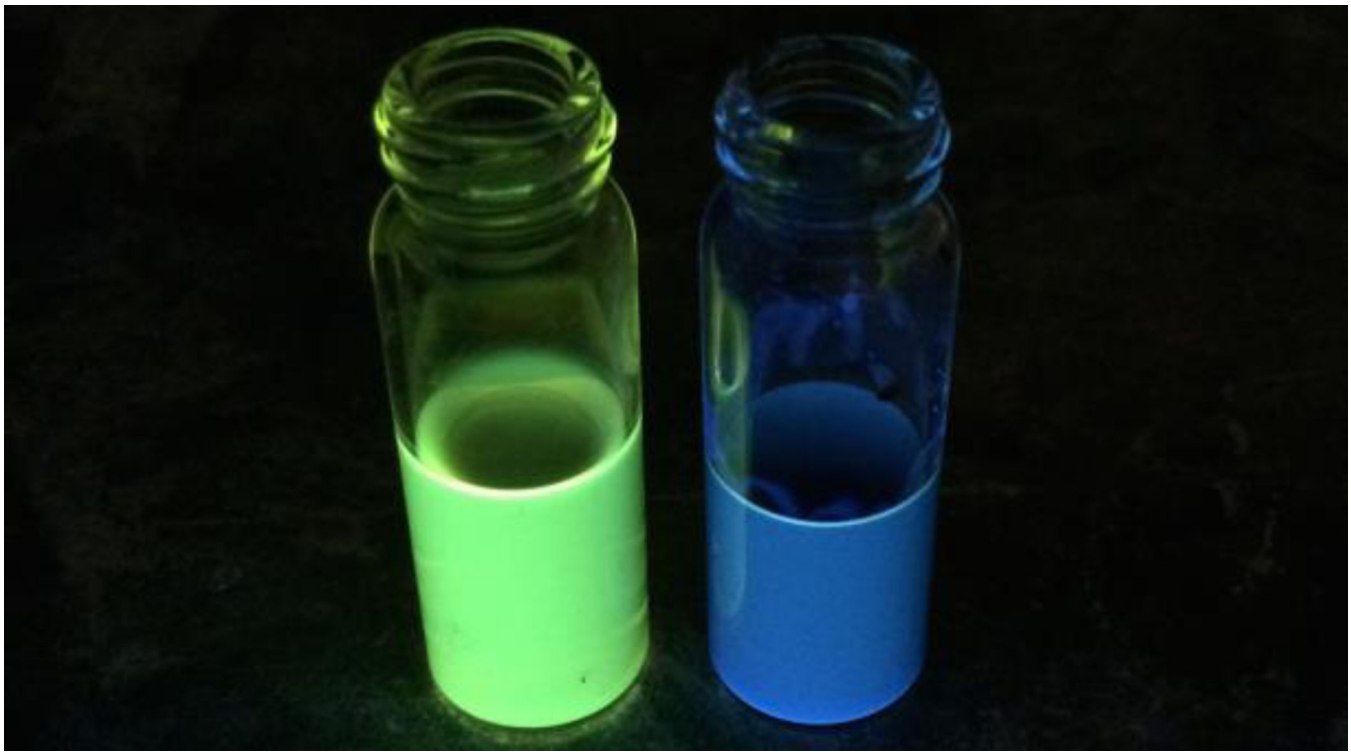

**Figure 3.**
Observed blue shift in emission upon protonation of **3b**.

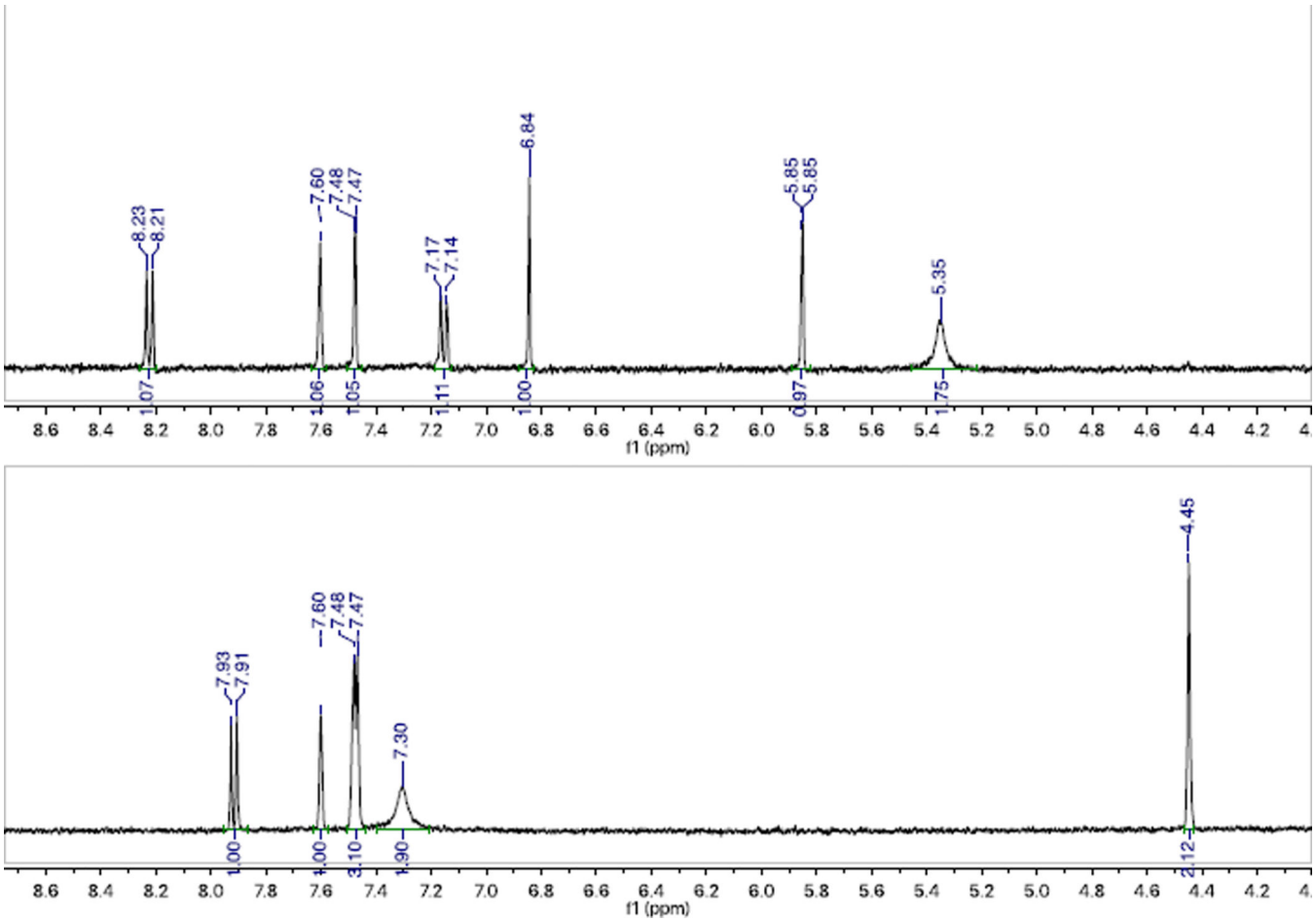


**Figure 4.**

NMR analysis of a) **3b** and b) **3b**– H+ (**T1** or **T2**) in CD3CN with 1.4 ppm upfield shift upon loss of aromaticity.

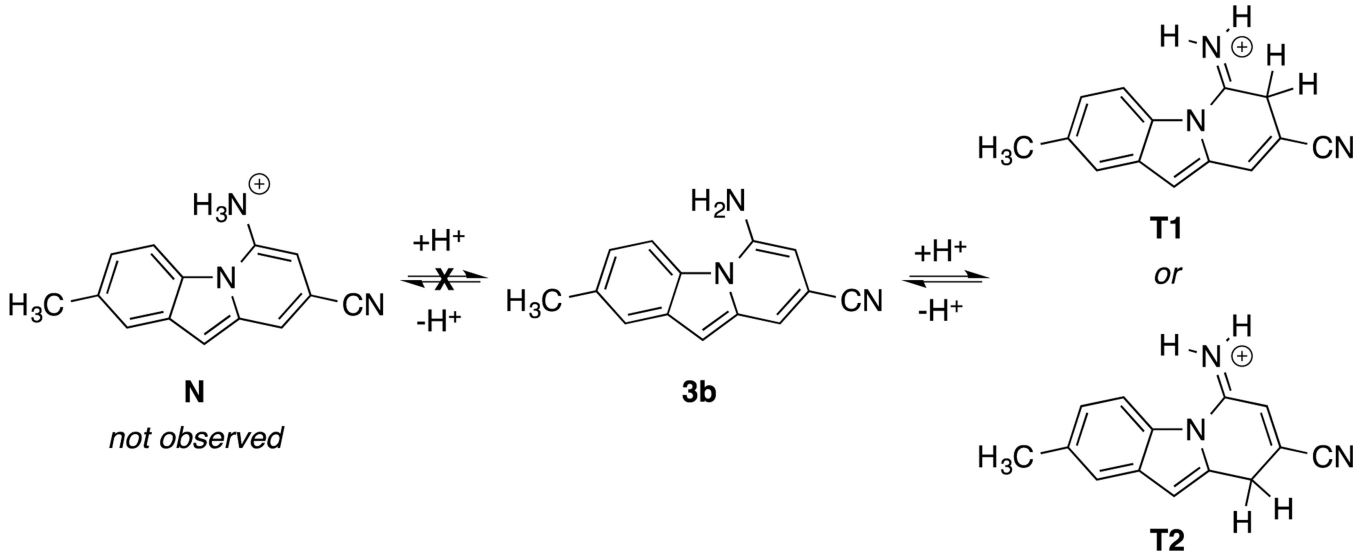


**Figure 5.**
Proposed protonated structures of **3b**.

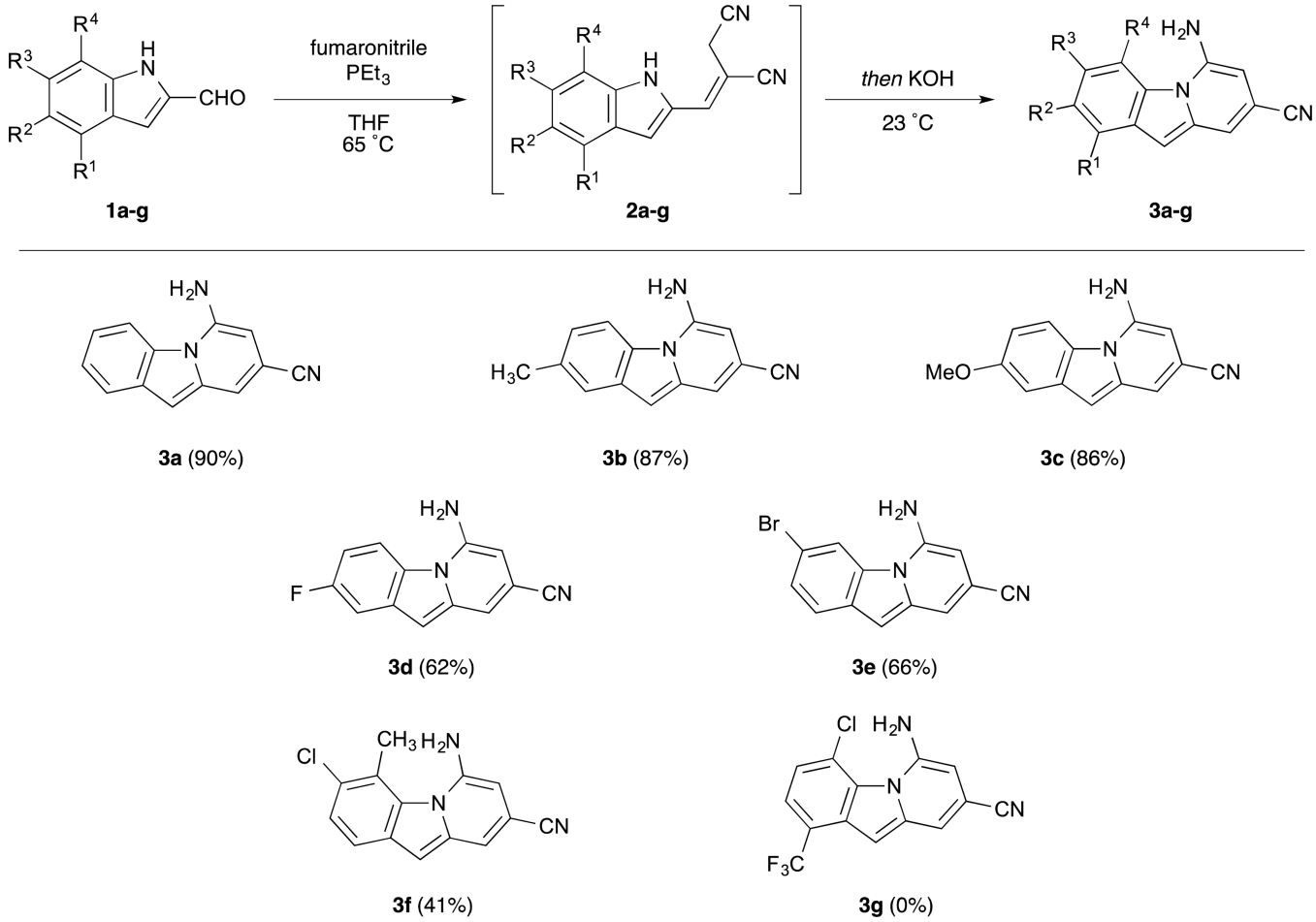


**Scheme 1.**

Scope of one-pot N–C cycloaromatization of substituted indole-2-carboxaldehydes to benzo[1, 2-*b*]indolizines.

**Table 1**

Photophysical Properties of Benzo[1,2-*b*]indolizines[a]

| compound | $\lambda_{max}$ (nm) | $\lambda_{em}$ (nm) | Stokes shift ($cm^{-1}$) | $\Phi_F$ |
|---|---|---|---|---|
| **3a** | 272, 338, 440 | 489, 517[b] | 2277 | 0.08 ± 0.01[b] |
| **3b** | 274, 335, 440 | 490, 527[b] | 2319 | 0.10 ± 0.01[b] |
| **3c** | 272, 339, 436 | 495, 526[b] | 2734 | 0.10 ± 0.01[b] |
| **3d** | 271, 333, 439 | 486, 516[b] | 2203 | 0.52 ± 0.07[b] |
| **3f** | 281, 358, 451 | 511, 535[b] | 2603 | 0.05 ± 0.01[b] |
| **3a**–$H^+$ | 362 | 428[c] | 4260 | 0.17 ± 0.01[c] |
| **3b**–$H^+$ | 370 | 442[c] | 4403 | 0.24 ± 0.01[c] |
| **3c**–$H^+$ | 377 | 498[c] | 6445 | < 0.01[c] |

[a] In $CH_3OH$.

[b] Excitation at 270 nm; tyrosine as standard.

[c] Excitation at 370 nm; quaterthiophene as standard.